2004-01-2323

Carbon Radiation Shielding for the Habot Mobile Lunar Base

Marc M. Cohen

Advanced Projects Branch, Space Projects Division, NASA-Ames Research Center

For permission and licensing requests contact:

SAE Permissions
400 Commonwealth Drive
Warrendale, PA 15096-0001-USA
Email: permissions@sae.org
Tel: 724-772-4028
Fax: 724-772-4891

SAE®

Global Mobility Database®

All SAE papers, standards, and selected
books are abstracted and indexed in the
Global Mobility Database.

For multiple print copies contact:

SAE Customer Service
Tel: 877-606-7323 (inside USA and Canada)
Tel: 724-776-4970 (outside USA)
Fax: 724-776-1615
Email: CustomerService@sae.org

Printed in USA

Carbon Radiation Shielding for the Habot Mobile Lunar Base

Marc M. Cohen

Advanced Projects Branch, Space Projects Division, NASA-Ames Research Center

ABSTRACT

Radiation is the leading showstopper for long duration human exploration of the lunar surface. The need for an effective and safe radiation shielding material has become the "Holy Grail" of radiation protection research. This paper reports the results for one material in particular – carbon – in the "Bioshield" particle accelerator test of candidate radiation shielding at Brookhaven National Laboratory, sponsored jointly by NASA and the Italian Space Agency. Shielding samples were bombarded by both Iron and Titanium nuclei beams at 1 GeV/n relativistic energy. This paper reports the results for Fe. The target behind the shielding was a lymphocyte culture; created using advanced cytogenetic techniques (premature chromosome condensation and fluorescence in situ hybridization). The shielding samples included aluminum, PMMA acrylic/Lucite, polyethylene, and lead.

The Habot Mobile Lunar Base Project at NASA-Ames Research Center provided the carbon-shielding sample because of its potential to provide a suitable shielding material to apply to the exterior of the Habot. The specific material tested is "CCAT CC-1, Carbon-filled carbon." This particular formulation has the advantage that the manufacturer controls the density to .01 g/cm^3. The density of this sample is 1.65 gm/cm^3. The carbon-filled carbon performed successfully, providing the second best dose reduction after polyethylene and the best overall reduction in radiobiological damage to the lymphocyte culture. This experiment suggests that carbon composites present important advantages for space habitat construction.

INTRODUCTION

 "Habot" is a contraction of habitat and robot. This introduction presents the Habot mobile lunar base, and three topics related to it: radiation, shielding options, and carbon shielding. The Habot concept involves a fully pre-integrated habitat module on the lunar surface with a mass budget of up to about 28% for externally attached radiation shielding. This shielding design would be specific to the Habot for the Galactic Cosmic Ray (GCR), Solar Particle Event (SPE), and secondary neutron risks and environment on the lunar surface.

An essential aspect of this research is that it grows from a specific project in architectural design research to solve the particular problem of providing radiation shielding for the Habot module during its mission on the lunar surface. It is not an effort to find the ideal radiation shielding material for all missions, modules, or applications. If other habitats, modules, or vehicles benefit from this research, that is a bonus, but it is not the criteria for success.

The ubiquitous requirement for the Habot is that it is mobile. This mobility requirement means that the shielding must be sufficiently compact and lightweight to not impede the design or versatility of the Habot module.

HABOT MOBILE LUNAR BASE

Mr. John Mankins, Director of Human and Robotic Technology in NASA's new Office of Exploration Systems, conceived the "Habot" Mobile Lunar Base concept (Mankins, 2000, 2001). The Habot is a module of 10 mTons that lands autonomously on the moon and walks or rolls to the base location. After multiple Habots land, assemble themselves into a base, and verify readiness, the crew arrives in a separate cislunar vehicle, the *Constellation* Crew Exploration Vehicle (CEV). They transfer to the Habot base, where they carry out the surface mission from roughly two weeks to two months. After the crew departs in the CEV ascent stage, the Habot base can disassemble itself and travel autonomously 100km or more to a new site of scientific interest. There, the Habots reassemble the base, connect, pressurize the port connections, and verify readiness and safety, the second crew lands in a CEV lander, The Advanced Projects Branch at NASA-Ames Research Center is working to substantiate the Habot as a candidate lunar surface base architecture (Cohen, 2003, 2004). Radiation shielding is a critical component of the Habot and any interplanetary vehicle or Mars surface habitat. FIGURE 1a and 1b show two such Mobile Base Concepts.
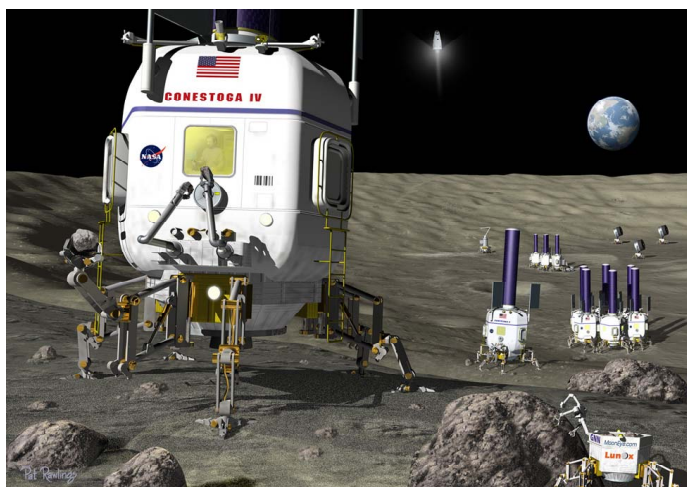
FIGURE 1a. Pat Rawlings' rendering of the "Habot" Mobile Lunar Base concept, courtesy of John Mankins, NASA HQ, and Neville Marzwell, JPL.
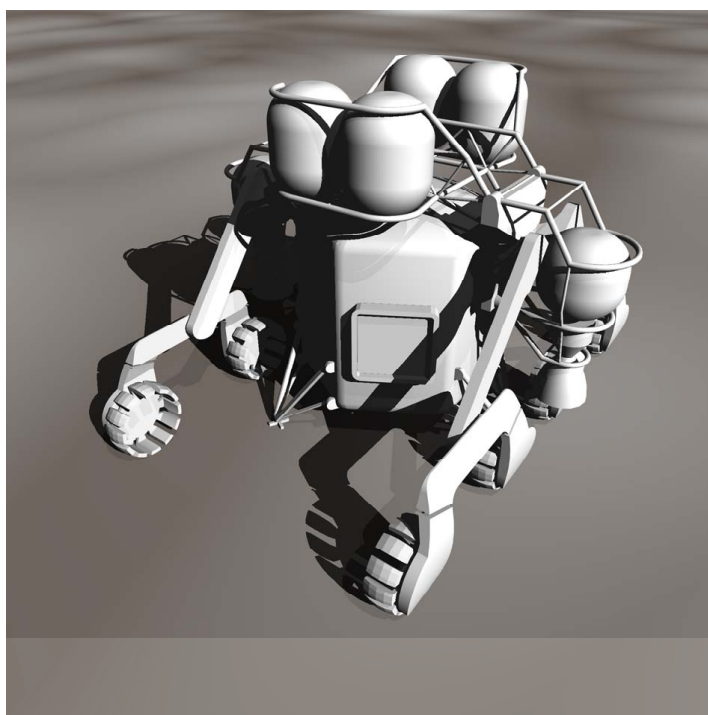

FIGURE 1b. Lai and Howe's "Mobitat" deployed to transport habitat module. By permission of A. Scott Howe.

RADIATION IN SPACE

Radiation is the leading showstopper for long duration human exploration of the lunar surface, interplanetary spaceflight, and Mars missions. Without an effective radiation shielding technology that supports the mission architecture within mass limits and radiation health-safety requirements, NASA simply cannot perform these missions safely with human crews. The radiation environment in space is complex, with a great variety of particles at a wide range of energies and velocities.

Professors Marco Durante, PhD, and Gianfranco Grossi, PhD, Dipartimento di Scienze Fisiche, Università "Federico II," Napoli, ITALIA, invited the author to contribute the carbon shielding sample to their funded NASA Research Announcement (NRA) experiment entitled "Space radiation shielding: biological effects of heavy ions after traversal of different shielding materials (experiment BIOSHIELD)." This science is supported and funded by the Italian Space Agency (Durante, 2001), and by NASA via the NASA Space Radiation Laboratory (NSRL). In their NRA proposal, Durante and Grossi's *Scientific Rationale* states:

> The exposure of astronauts to the cosmic radiation poses a major risk to space flights, especially the interplanetary missions (NASA Life Sciences Division, 1999). One of the major problems in estimating radiation risk for astronauts is the uncertainty of the actual particle distribution at the point of exposure of crewmembers, or actually, at the site of specific organs inside the body.... high-energy particle radiation in space is very penetrating. A thin or moderate shielding is generally efficient in reducing the equivalent dose, but as the thickness increases, shielding effectiveness drops. This is the result of the production of a large number of secondary particles, including neutrons, caused by nuclear interactions of the galactic cosmic rays (GCR) with the shielding. These particles have generally lower energy, but can have higher quality factors than incident primary cosmic particles.

These quality factors make all the difference in risk for potential health effects.

The radiation-shielding problem for the Moon consists of two sources: primary particles and secondary neutrons. The primaries consist of galactic heavy ions, solar protons, and other solar particles. The secondary neutrons come from "back scatter" when the primaries strike both the habitat and the lunar regolith. Dosages of these ionizing particles in excess of allowable dose limits can impair, permanently injure, or even kill a crew.

Radiation modeling and laboratory experiments have led to several important discoveries about radiobiological effects, shielding performance and the interaction of these two factors. Among the primary radiation sources, the heavy ions (mostly the nuclei of **C**, **Fe**, **He**, **Mn**, **Ne**, **Ti**, and **Xe** – please refer to TABLE 1) pose the greatest danger of direct biomedical damage – by a quality factor of approximately 30 greater than the equivalent absorbed dose of other radiation types (protons, gamma, x-rays, neutrons, etc). Thus, it is vital to reduce the incident doses of these primaries.

REVIEW OF SHIELDING OPTIONS

The traditional options for shielding are confined to a handful of materials, all of which have shortcomings in certain properties and performance characteristics. These options fall into two categories: practical shielding and In Situ Resource Utilization shielding.

Traditional and Practical Shielding -- The traditional shielding options include, first of all aluminum-the most commonly used aerospace structural metal, and materials that are better absorbers of energy and lesser emitters of secondary neutrons than aluminum. These materials include the small selection of water, polyethylene, Lucite (polymethyl methylacrylate – PMMA).

Water is a unique case, because it has the advantage of being amorphous, such that a habitat could be launched with tank shields empty to reduce launch mass. Those tanks could be filled with water later on orbit, or on the lunar or Mars surface (Cohen, 1996, 1997). If it is possible to extract water from the environment, there may be practical advantages to a water shield.

All of these shielding materials come with cost, mass, and volume penalties, and none of them are satisfactory as an *engineering solution* for the Habot. As elaborated below, **Al** is an unacceptable producer of secondary neutrons and is also too heavy for the Habot mass budget. Because the habitable volume inside the Habot will be very tight, it will be essential to install the shielding on the exterior, where it may also perform multiple functions such as thermal insulation, and micrometeoroid shielding. None of the good energy absorber/low neutron emitter materials (Water, polyethylene, Lucite) possess the structural and thermal properties to allow them to be installed on the exterior of a Habot.

Regolith ISRU Shielding -- One concept that space exploration visionaries have proposed for decades is to use lunar or martian regolith as a shielding material. Lunar regolith is a net emitter of neutrons, so the shielding layer of regolith is often proposed as 1m or thicker. This in situ resource utilization (ISRU) approach would save the weight penalty of transporting shielding material to the Moon or Mars. However, to prepare and apply regolith shielding to a surface habitat would impose tremendous demands upon the mission architecture and operations. It would require heavy excavating equipment, a bagging machine, and a machine to move and emplace the bagged regolith. From an exploration perspective, the greatest cost of regolith shielding may be the complete loss of mobility to the shielded habitat module.

Visionary Shielding -- There are various proposals for theoretically efficacious but currently impractical shielding materials such as solid hydrogen, liquid hydrogen, liquid oxygen, and electromagnetic fields. All these macro-shielding schemes suffer from essentially the same obstacles. The all require a huge, massive, complex and costly infrastructure that consumes vast amounts of energy. There are also significant physical integration problems, such as building pressure port hatches and windows that pass through cryo-cooled **H** or O_2, or protecting microelectronics in the habitat from powerful magnetic fields outside. The specifics of some of these visionary approaches are discussed below, in the "little walk through the periodic table."

Need for a Shielding Alternative – This brief review of shielding options establishes that existing technologies do not provide a satisfactory shielding material for the Habot. It became necessary to seek an *engineering solution* that would answer the above design requirements and objections to conventional options.

CARBON SHIELDING

The rationale for testing **carbon** as shielding include the low atomic number and weight, temperature range, and structural properties:

1. Z/A -- The ratio of Atomic Number over Atomic Weight (Z/A) is a first order predictor of secondary neutron production. Hydrogen is the best, with one proton and no neutron, for a "perfect" value of 1. Polyethylene, which is rich in **H,** has a Z/A of .571. **C-12,** with 6 protons and 6 neutrons, has a Z/A of .5. Al –27 with 13 protons and 14 neutrons has a Z/A .48, which is not a big difference numerically, but does signify one "excess" neutron. Although the Z/A ratio is the primary attribute, a simplified way to think about neutron producers is simply by the Z, atomic number itself. The smaller the Z, the lesser the potential for "excess neutrons" in the common isotope of an element. Following this view, Carbon has the atomic number 6, which is considerably lower than aluminum, atomic number 13, and so would be a better blocker of primary particles and produce a smaller number of secondary neutrons.

2. External Application and Temperature Range --The Habot crew living environment will be quite small in each module, with a diameter from 3.5 to 5.0m in diameter. It will be most advantageous to be able to install shielding on the exterior of the Habot module rather than on the interior. Polyethylene has been the preferred supplemental shielding material for ISS; however, polyethylene cannot tolerate the extreme temperature swings of the lunar day-night cycle. Carbon-carbon can easily tolerate the extreme thermal cycling of the lunar day and night, and so can be applied to the exterior of the Habot, which is not possible with water or polyethylene.

3. Neutron Emission and Non-Metallic Material -- Since aluminum appears to be problematic as a shielding material because of the neutron backscatter, NASA may need to find an alternate material from which to build human spacecraft. If it proves desirable to develop an aluminum-free habitat module, it will be possible to craft multi-functional exterior layers from carbon materials that perform the same purposes that aluminum alloy now serves. These functions include a carbon composite pressure vessel, carbon foam (developed by the Ultramet Corporation and carbon-carbon thermal insulation thermally conductive carbon radiators (developed at Oak Ridge National Lab).

This paper describes the implications of the findings for all the material samples in general, and those of the carbon sample in particular, for use as exterior shielding on the Habot.

THE SPACE RADIATION ENVIRONMENT

GCRs are the most potent and damaging species of particle radiation in space. Iron nuclei are of particular interest for radiation shielding research and engineering because they are among the most powerful and damaging part of the GCR radiation flux in space. This investigation considers both the "free space radiation environment" and the Solar Particle Event. The design assumption is that shielding effectively against GCRs for a long duration exposure will confer a suitable measure of protection against SPEs. If further analysis shows that a "solar storm shelter" is required, the working assumption is that it would be a small volume that would contain the crew in very close quarters, enclosed by a greater thickness of the optimum shielding material.

GRAPH 1 shows the distribution of particles in space across the energy spectrum of the "free space radiation environment (Simonson, Nealy, 1991, p. 2-3). Notice that the highest energy particles are the GCRs, in the energy range of 10^2 to 10^4 MeV (Simonson, 1997). Iron (**Fe**) nuclei fall within to the middle to upper end of this range. The experiment described in this paper concerns Fe particles traveling at the relativistic energy and speed of 10^3 MeV/n, which equals 1 GeV/n.

SO, WHY IRON NUCLEI?

GRAPH 2a shows the relative abundance of GCR particles as a function of the Atomic number, Z. Generally, reading GRAPH 2a from left to right, the most abundant particles are those with the smallest mass. The particle abundance decreases with increasing Z.

Graph 2a shows a sharp spike upward in abundance at Z=26, the atomic number of **Fe** – the "iron spike" shown in the red circle. In terms of particle "impact," this **Fe** spike is very significant because it means that it is a very heavy particle with a order of magnitude – ten times higher -- abundance than its neighbors in the Periodic Table. The radiobiological effect (RBE) that a particle can do is directly proportional to both its energy and its mass. Therefore Fe is of particular concern as a cause of RBE, particularly cell death (Sapp, Philpott, et al, 1992) and cell transformations that lead to an increased risk of cancer.

GRAPH 2b presents the differential flux of four GCR particles as a function of kinetic energy **H**, **He**, **C**, and **Fe**. Please see TABLE 1 for the relative position of these elements in the Periodic Table. All four occur on the top line of their Group (column). However, **H** and **He** reside in the top row; **C** resides in the second row, and **Fe** resides in the fourth row. Their relative positions on the Periodic table portray in a visual and dramatic way the corresponding difference in mass.

KINETIC ENERGY

The Newtonian formula for Kinetic Energy, K, is $K=1/2MV^2$. For a GCR particle, energy in MeV translates into velocity. If an **H** particle (one proton) and an **Fe** particle with 26 protons and 29 neutrons carry the same energy, at say 10^4 MeV/n, the **Fe** particle has 55.85 times more "hitting power" than the **H**. This "hitting power" means that a **Fe** particle carries much greater potential to damage or kill cells. It also means that a **Fe** particle has much greater potential to backscatter secondary neutrons from a material that it hits such as shielding or human tissue. Finally, the **Fe** particle has the potential to shed neutrons that become scatter.

SHIELDING PROPERTIES

From the perspective of absorbing LET, the ideal material is abundant in loosely bonded hydrogen atoms which absorb the most LET. **H** has no neutron except in the rare deuterium and tritium isotopes. (Please refer to TABLE 1, the periodic table of the elements for the following discussion.)

The binding energy per nucleon curve peaks at **Fe-56** with about 10 MeV/nucleon binding energy. **Fe-56** has the greatest binding energy per nucleon and is the hardest to extract particles from its nucleus. However, its ratio of neutrons to protons is 30/26 (1.15385). In a relativistic collision with a projectile energy of 10's of MeV to 100's of GeV per nucleon, a projectile of **Fe-56** will generate extra neutrons that have long mean free paths lengths. This collision will also generate protons and other charged fragments, but they will dissipate energy through LET collisions; neutrons will not (personal communication, Robert Singleterry, April, 2004).
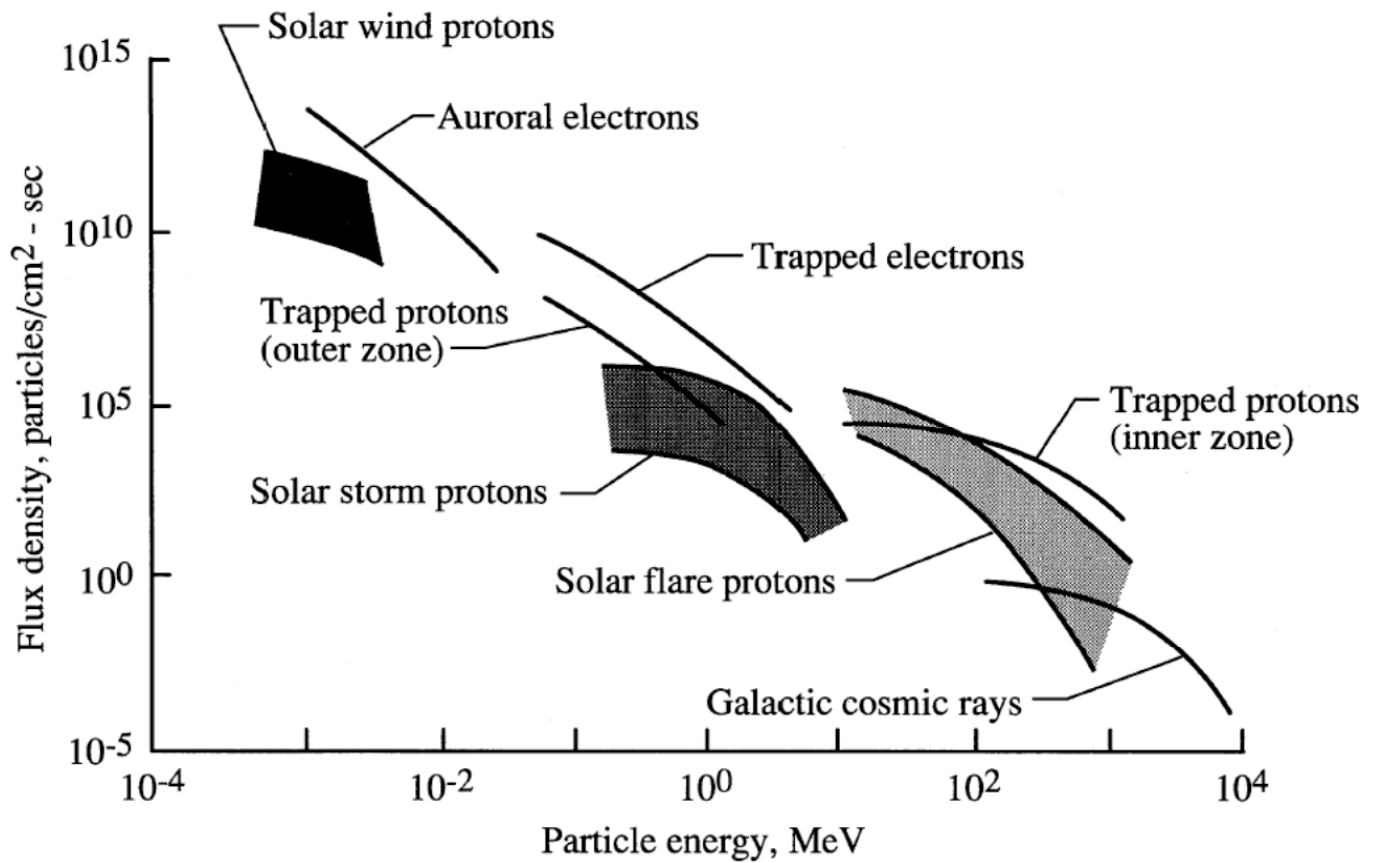
GRAPH 1. Free space radiation environment as flux density vs. particle energy. Source: Simonson, Nealy, 1991; Simonson, 1997; after Wilson, 1978. (Courtesy of Robert Singleterry, LaRC).
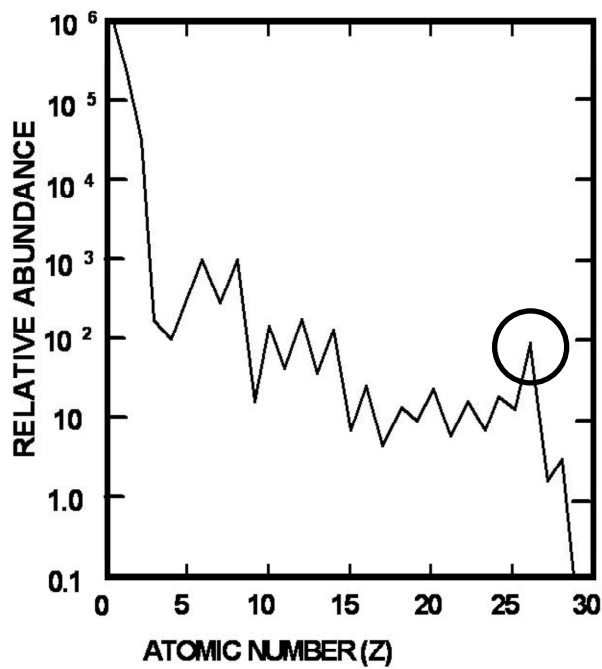
GRAPH 2a. Relative abundance of GCR particles as a function of Atomic Number, Z. Source: John W. Wilson, et al, LaRC, (1998). The "iron spike" occurs at Z=26.
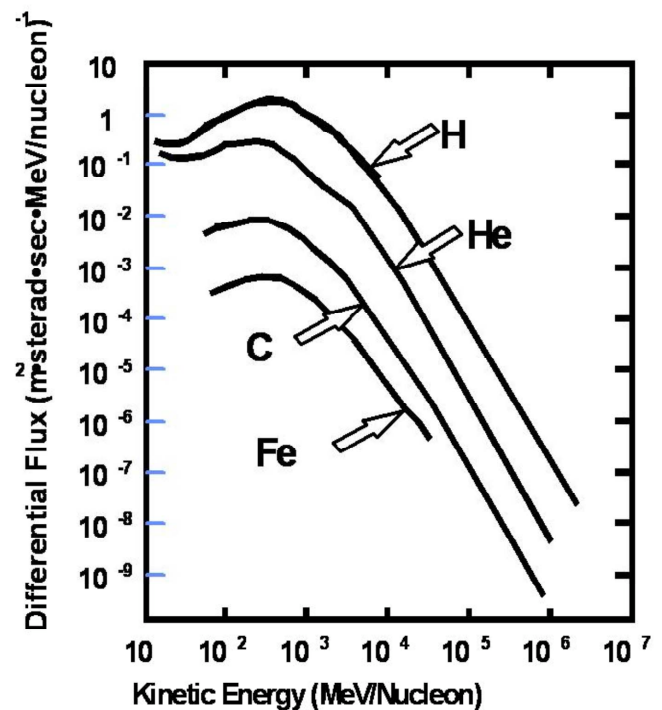
GRAPH 2b. Differential flux of Four GCR particles as a function of Kinetic Energy. Source: John W. Wilson, et al, LaRC, (1998), (courtesy of Robert Singleterry, LaRC.)

Group**

Period	1 IA 1A	2 IIA 2A	3 IIIB 3B	4 IVB 4B	5 VB 5B	6 VIB 6B	7 VIIB 7B	8	9 VIII 8	10	11 IB 1B	12 IIB 2B	13 IIIA 3A	14 IVA 4A	15 VA 5A	16 VIA 6A	17 VIIA 7A	18 vIIIA 8A
1	1 H 1.008																	2 He 4.003
2	3 Li 6.941	4 **Be** 9.012											5 B 10.81	6 **C** 12.01	7 N 14.01	8 O 16.00	9 F 19.00	10 Ne 20.18
3	11 Na 22.99	12 Mg 24.31											13 **Al** 26.98	14 Si 28.09	15 P 30.97	16 S 32.07	17 Cl 35.45	18 Ar 39.95
4	19 K 39.10	20 Ca 40.08	21 Sc 44.96	22 Ti 47.88	23 V 50.94	24 Cr 52.00	25 Mn 54.94	26 Fe 55.85	27 Co 58.47	28 Ni 58.69	29 Cu 63.55	30 Zn 65.39	31 Ga 69.72	32 Ge 72.59	33 As 74.92	34 Se 78.96	35 Br 79.90	36 Kr 83.80
5	37 Rb 85.47	38 Sr 87.62	39 Y 88.91	40 Zr 91.22	41 Nb 92.91	42 Mo 95.94	43 Tc (98)	44 Ru 101.1	45 Rh 102.9	46 Pd 106.4	47 Ag 107.9	48 Cd 112.4	49 In 114.8	50 Sn 118.7	51 Sb 121.8	52 Te 127.6	53 I 126.9	54 Xe 131.3
6	55 Cs 132.9	56 **Ba** 137.3	57 La* 138.9	72 Hf 178.5	73 Ta 180.9	74 W 183.9	75 Re 186.2	76 Os 190.2	77 Ir 190.2	78 Pt 195.1	79 Au 197.0	80 Hg 200.5	81 Tl 204.4	82 **Pb** 207.2	83 Bi 209.0	84 Po (210)	85 At (210)	86 Rn (222)
7	87 Fr (223)	88 Ra (226)	89 Ac~ (227)	104 Rf (257)	105 Db (260)	106 Sg (263)	107 Bh (262)	108 Hs (265)	109 Mt (266)	110 --- 0	111 --- 0	112 --- 0		114 --- 0		116 --- 0		118 --- 0

Lanthanide Series*	58 Ce 140.1	59 Pr 140.9	60 Nd 144.2	61 Pm (147)	62 Sm 150.4	63 Eu 152.0	64 Gd 157.3	65 Tb 158.9	66 Dy 162.5	67 Ho 164.9	68 Er 167.3	69 Tm 168.9	70 Yb 173.0	71 Lu 175.0
Actinide Series~	90 Th 232.0	91 Pa (231)	92 **U** (238)	93 Np (237)	94 **Pu** (242)	95 Am (243)	96 Cm (247)	97 Bk (247)	98 **Cf** (249)	99 Es (254)	100 Fm (253)	101 Md (256)	102 No (254)	103 Lr (257)

As an analogue, the fission process relies on the liberation of neutrons to sustain a chain reaction. Typically, this process uses **U-235** for a controlled fission reaction. However, the **U-238** isotope, with three more neutrons, emits a higher number of neutrons during radiothermal decay. (Personal communication via e-mail, Robert Singleterry, April 27, 2004; personal conversations with Marcus Murbach, April, May 2004).

IDEAL RADIATION SHIELDING

From these observations, the ideal (but alas, not "perfect") shielding material would be a low atomic number that is solid and stable at "room temperature," and has useful material and structural properties. Foremost among these properties would be chemical stability, a wide temperature range, non-toxicity, structural strength, and is affordable in the quantities needed -- about 2800kg per one Habot (Cohen, 2003, p. 8).

Given the 10,000kg ceiling on the Habot module mass (Cohen, 2003), the allocation of 28 percent for shielding in the mass budget is a unique departure – the first time that any pragmatic spacecraft proposal dedicated so much mass for radiation protection. What this large mass fraction implies is that the shielding mass must perform multiple functions. These functions may include structural capacity as a pressure vessel, thermal insulation, thermal heat rejection (from a body-mounted radiator), micrometeoroid protection, and perhaps even photovoltaic power generation from solar energy.

A LITTLE WALK THROUGH THE PERIODIC TABLE

A quick walking tour from the top of the period table will present the pragmatic Aerospace Architecture view of "low-Z" elements as candidate materials for radiation shielding. The walk leads to **C** (Atomic Number 6) as the first element that can possibly satisfy these requirements. It continues on to **Al** (13), which is the most common preferred aerospace structural metal. This "walk" also shows that there is not anything clever about carbon as a shielding material. Indeed, it should be self-evident.

1. Hydrogen (**H-1**), as stated above, is the ideal shielding material. However, H is a gas at ambient temperatures, and so is not practical in that phase as shielding. There are a variety of fantasies to create solid H. However, a solid hydrogen structure is utterly impractical because the technology does not exist to create and maintain it at close to absolute zero° K. In addition, the energy source would not be available to keep a large hydrogen structure frozen, or to contain liquid H in a cryogenic pressure vessel around a space habitat.

Some of the newest proposals involve containing liquid H at cryogenic temperatures in carbon nanotubes under extremely high pressure in a non-cryogenic pressure vessel around a habitat. However, the practical difficulties are too great at this time for maintaining the crew's living environment inside this double or triple pressure vessel. These practical questions include providing pressure ports and hatches for crew access and egress, windows, electrical and data cables, and thermal conductors penetrating through the successive pressure vessel shells. In addition, at this time, carbon nanotubes are still an extremely scarce commodity. The cost is roughly $1,000,000 per kilogram and usually it is available commercially only in microgram quantities.

2. Helium (**He-4**) is a gas at ambient temperatures. It sits at the top of the noble gas family, and does not combine readily with other atoms to form any other molecules of potential structural value, and so is not practical as shielding.

3. Lithium (**Li-7**) is solid at ambient temperatures, however, it has a low melting point of 180.5°C, is highly reactive chemically, particularly with water, and it corrodes easily. It is not practical as shielding by itself, but Singleterry and Thiebeault (2000, p. 3) comment that the Li-6 isotope can be added to polyethylene or other (carbon and hydrogen) compounds as a neutron absorber.

4. Beryllium (Be-9) is solid at ambient temperatures, and has one of the highest melting points of any metal at 1287°C. However, "It has a high permeability to X-rays and when bombarded by alpha particles, . . . neutrons are produced in the amount of about 30 neutrons/million alpha particles" (LANL, 2004). Beryllium is highly toxic and very difficult to machine in its unalloyed, elemental form. A **Be** MSDS states: "Incompatible with acids, bases, oxidizing agents, halogen compounds, halogens, alkali metals." When alloyed with aluminum, it is still a minority constituent, and so does not mitigate the properties of aluminum significantly. **Be** would not be helpful or practical as a shielding material.

5. Boron (**B-10**) The Boron-10 isotope has applications as shielding in nuclear power reactors, where it is useful primarily as a low-energy neutron absorber. However, **B-10** is not abundant compared to B-11, and does not occur naturally in exploitable quantities, and so requires extensive, rather expensive processing to produce it in "commercial quantities" at the scale of microchips. **B-10** has a Z/A of 0.5. It has a very high melting point of 2075°. Boron may have some very useful applications to future advanced composites or polyethylenes. Robert C. Singleterry, Jr., and Sheila A. Thibeault of NASA-LaRC state:

> "Additives to the basic polyethylene base [sic] have some effect on the integral shielding properties. For example, if an efficient neutron absorber is added, like B-10, then the total number of transmitted neutrons is reduced by another 10 percent . . .. It is worth noting that of the polyethylene-based materials, the B-10 material produced the smallest integrated reflected flux, probably because the number of neutrons available for the scattering reaction channel is reduced because of the high absorption" (Singleterry, Thibeault, 2000, p. 3).

6. Carbon (**C-12**) occurs in three pure elemental forms at ambient temperatures – diamond, graphite, and buckminsterfullerene-60. Graphite and its various preparations as composites offer potential advantages as a shielding material. It has a wide temperature range and excellent structural properties so it can be attached to the exterior of a pressurized module. Carbon composites are well within current technology. The Z/A is 0.5, the same as for **B-10**, an excellent neutron

absorber. Following the walk through the Periodic Table, this paper discusses the case for carbon shielding in greater detail.

Continuing the march through the Periodic Table, it becomes apparent that the next suitable material for spacecraft construction is Aluminum:

7. Nitrogen (**N-14**) is a gas at ambient temperatures.

8. Oxygen (**O-16**) is a gas at ambient temperatures. As a cryogenic liquid, it may serve as a good shield, but that encounters the same problems as a liquid hydrogen shield.

9. Fluorine (**F-19**) is a gas at ambient temperatures and highly toxic, corrosive to human skin, and reactive with many other substances.

10. Neon (**Ne-20**) is a gas at ambient temperatures.

11. Sodium (**Na-23**) Sodium is a potent alkali metal that reacts violently with water. It is extremely reactive and lacks structural properties, and so is not a practical shielding material.

12. Magnesium (**Mg-24**) in its elemental form is extraordinarily flammable in the presence of O_2. An MSDS for **Mg** states:

> J.T. Baker SAF-T-DATA (tm) Ratings
> Flammability Rating: 3 - Severe (Flammable)
> Reactivity Rating: 3 - Severe (Water Reactive)

Mg is used in alloys of aluminum for aircraft and missile structures, but usually in such minority proportions as to have little effect in changing the shielding properties of aluminum. **Mg** does not afford useful shielding properties for Habot.

13. Aluminum (**Al-27**), the most common material in use today for pressure vessel structure, interior racks, and many other items, is a ferocious emitter of secondary neutrons. These secondary neutrons can cause more biological damage than the primaries that triggered them. However, aluminum, the most common material in use today for pressure vessel structure, interior racks and many other items, is a ferocious emitter of secondary neutrons. Townsend, Nealy, Wilson & Simonson (1990, p. 8-9 show that neutrons *increase* dramatically in direct proportion to the thickness of an aluminum shield. These secondary neutrons can cause more biological damage than the primaries that triggered them. In a computational simulation, Singleterry and Thiebeault (2000) found a high rate of neutron backscatter from **Al** bombarded by low-energy neutrons above 1 MeV. (Personal communications with Robert Singleterry, Jr., NASA LaRC, March and April 2004) Based on this

precept, the author's predicted result for this experiment was that the relativistic dose reduction data for each shielding material would predict the biological effects. In a Habot approximately 5m in diameter by 5m in height, this shielding thickness would demand 16,800kg of **Al**, which is a non-starter for a 10,000kg mass budget.

Beyond **Al**, lead (**Pb**) is a good X-ray shield and a passable low energy neutron shield. However, for space applications **Pb** has several shortcomings. It has a low melting point, poor structural qualities, and is toxic when absorbed in the human body. When bombarded by relativistic particles, lead can be a net neutron emitter. Measured as a unit of shielding efficacy per unit mass, lead is not efficient compared to a number of other materials. Lead is not suitable for space radiation shielding.

Further down the Periodic Table, a potentially more promising neutron absorber is hafnium (**Hf**), which is the key material used to make the control rods in nuclear fission reactors. **Hf** is such a good absorber of low-energy neutrons produced by fission that inserting the control rods into the reactor core slows down the reaction. The reactor safety design is based upon the complete insertion of the **Hf** control rods stopping the fission reaction entirely.

THE CASE FOR CARBON

A collaboration between researchers at NASA-LaRC and the NASA Center for Applied Radiation Research (NCARR) at Prairie View A & M University simulated shielding materials bombarded by neutrons. They produced important results that appear in TABLE 2.

The significance of TABLE 2 is multifold. First, it shows the substantial difference of the metallic shields – aluminum and titanium – from the lower atomic number materials – polyethylene and epoxy composite. Al and Ti reflect significantly fewer neutrons from the "front side" of the shielding than the other materials. Thus, it is not surprising that Al and Ti transmit considerably more neutrons through the shielding, while also producing an additive "backscatter" of neutrons. In terms of overall flux reduction, the polyethylenes perform best, followed by the composite, which is about 84 to 87 percent as effective as the polyethylenes. From the composite to the aluminum, there is performance gap that is roughly twice as large as the gap from polyethylene to composite. The titanium produces yet another, larger performance gap.

What is the difference between the metallic and non-metallic shielding materials? The elemental metals are larger atom, with many more neutrons. The polyethylenes and composite contain smaller atoms with fewer neutrons. The polyethylenes and the composite all contain both hydrogen and carbon, but the relative

proportions vary. TABLE 3 shows the relative proportions of these constituent elements.

Taken together, what TABLES 2 and 3 show is that hydrogen is the most significant element, both in terms of reflected and reduced transmission of neutrons. However, the epoxy composite at 73.8 percent carbon performs virtually as well as the polyethylenes as a neutron reflector. The difference in reducing transmission of neutrons arises because hydrogen is a superior absorber of neutrons for two reasons. First, the loosely bonded H atoms can absorb more linear energy transfer (LET) from energetic neutrons than the more structured epoxy composite molecules. The boronated polyethylene is superior as a reducer of neutron transmission (by about 10 percent) because Boron-10 is an excellent neutron absorber. Second, the hydrogen atom does not normally have a neutron. The transmission data cannot distinguish between primary neutrons and secondary neutrons; some neutrons may be produced within the composite itself.

TABLE 2. Transmitted and Reflected Neutron Flux from Each Material per Source Neutron Computational Simulation. All shielding materials were $3 g/cm^2$ (adapted from Singleterry, Thiebeault, Wilkins, Huff, 2002, p. 7).

Material	Reflected Flux #/cm²-sec-source	Transmitted Flux #/cm²-sec-source	Reduction in Transmitted Flux as percent of Unshielded Flux, D_R
Unshielded Source	N/A	4.302e-2	0%
Aluminum (2024 Al Alloy)	4.946e-2	1.904e-2	55.75%
Polyethylene	5.361e-2	0.962e-2	77.63%
Boronated (B-10) Polyethylene	5.187e-2	0.850e-2	80.24%
Epoxy-Carbon Composite (AS4/3502)	5.182e-2	1.381e-2	67.89%
Titanium (Ti 6A14V Alloy)	4.848e-2	2.249e-2	47.72%

TABLE 3. Fractional Composition of Polyethylene and Epoxy Composite in percent (adapted from Singleterry et. al., 2002 p. 6).

Material	H	C	B-10	Other
Polyethylene	66.8	33.2	-	-
Boronated Polyethylene	62.5	31.0	6.5	-
Epoxy Composite	21.4	73.8	-	5.8

The Department of Energy (DOE) defines four energy levels for radiation particles: thermal, low-energy (slow), high-energy (fast) and relativistic. The data available above for carbon as a component of shielding above derives from the low-energy range between 10^{-3} MeV and 20 MeV. The relativistic energy range is the level of concern for GCRs, 1 GeV/n and above. It is not good physics to use the low-energy data to predict specific results at relativistic levels, nor to generalize from neutrons to nuclei. However, the low-energy results for **C** are most suggestive, and so led to the investigation of a carbon shielding sample in a relativistic particle beam.

OBJECTIVES

For the Habot Project, the objective is so simple as to hardly qualify as science: to test a candidate carbon-carbon composite under simulated space GCR radiation conditions. For Durante and Grossi and their supporting agencies, the objectives are far more sophisticated and complex. They will be publishing their results in the relevant journals. In their NRA proposal, they point out that most of the uncertainty associated with radiation exposure derives from the biology, and thus there is a need for biological assays of radiation damage. Specifically, they cite the recognized need to evaluate "cell-killing and chromosomal aberrations . . . as a function of the thickness and composition of shielding" (National Academy of Science, 1996).

The Bioshield experiment is based upon several types of research. Ballarini et al (1999) conducted computer simulation of light ion effects on chromosomes and DNA. Durante, Furusawa, and Gotoh (1998) presented a method for chromosome analysis as a basis for biodosimetry, "to find a simple protocol for measuring chromosome damage." The connection between cancer risk and chromosomal aberrations has been substantiated by epidemiological studies (Durante, Bonassi, George, Cucinotta, 2001, p. 662). These researchers explain the purpose of investigating this connection:

"There are many advantages in using chromosomal aberrations for monitoring cancer risk within individuals exposed to cosmic radiation: (1) An increased level of chromosomal aberrations indicates potential cancer risk that

cannot be detected using the classic epidemiological approach. (2) Chromosomal aberrations are early events in the pathway linking exposure to cancer; therefore, intervention based on this biomarker offers a potential for prevention. (3) The large interindividual variability observed in biomonitoring studies can be used to identify subjects who are particularly susceptible to radiation damages and are therefore at high risk of cancer" ((Durante, Bonassi, George, Cucinotta, 2001, p. 666).

The Bioshield experiment measures four "biological endpoints" to human lymphocyte cultures exposed to unshielded and shielded Fe and Ti particle beams at relativistic energies: 1 GeV/n (Durante, Grossi, 2002, NRA Proposal). The four biological endpoints proposed for study are:

- Survival, delayed reproductive death, and neoplastic transformation of HeLaxSkin Fibroblasts
- Chromosomal aberrations in human peripheral blood lymphocytes
- Cell killing and mutation induction in human lymphoblasts
- DNA fragmentation spectra in human diploid skin fibroblasts.

This paper presents preliminary results for chromosomal aberrations due to bombardment by 1 GeV/n Fe ions through the several shielding materials.

APPROACH

In FY2003, the Habot Project received funding from Mr. Mankins, to develop an advanced composite shielding material that would be lightweight, have structural strength and stability, have a wide temperature range and offer superior properties to attenuate particle energies while minimizing secondary neutron generation. After reviewing a wide range of candidate materials, the Habot Project selected "carbon-filled carbon" for a radiation shielding experiment at Brookhaven National Lab (BNL), in Upton, NY. We got our "Beam Time" at BNL on November 10, with 1GeV/n exposures of **Fe** and **Ti** nuclei.

The **C** shielding research began with a survey of commonly available carbon composite materials. The survey considered a wide variety of carbon-carbon composites (such as the black RCC panels on the Space Shuttle leading edge) in the range of ~1.0g/cm^3 to ~2.5 g/cm^3). It also considered lighter weight, lower density carbon materials with appropriate thermal and structural properties such as vitrified carbon foam ~.05 gm/cm^3 to .50 gm/cm^3). In addition, some alternative "filler" type materials such as aero gel were also candidates. This survey involved products from a variety of manufacturers.

While these comparisons proved educational on their own merits, that level of detail is not appropriate for this discussion.

FIGURE 2a. Gianfranco Grossi (l) Co-I and Marco Durante, P-I, University Frederico II, Naples, Italy, set up one 5gm/cm^2 Carbon-filled Carbon panel for the beam test at BNL. By permission of Grossi/Durante.
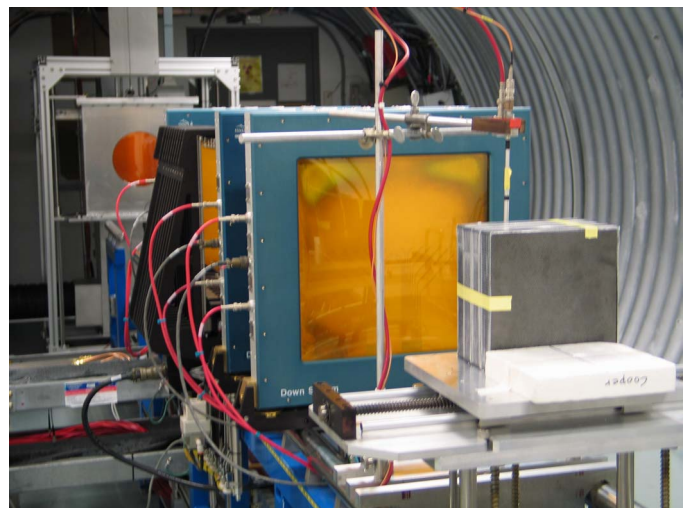

FIGURE 2b. 4 Carbon-filled Carbon panels comprising 20gm/cm^2 set up in line for the beam test. By permission of Grossi/Durante.

SELECTION OF MATERIALS

The challenge for the author was that there was sufficient budget and time to fabricate and test only one carbon material as a radiation-shielding sample. Meeting the dimensional constraints provided by Durante and Grossi for the experiment set up at BNL proved to be a determining factor. The experimental design called for testing sample materials in two mass thicknesses: 5 gm/cm^2 and 20 gm/cm^2. The maximum allowable front to back thickness was understood to be 15 cm. This

inferred thickness constraint precluded the lower density candidates such as vitrified foam that would exceed the 15cm front to back limit for the 20 g/cm^2 specimen (however, for future experiments, a longer stage will be available to test less dense materials).

With the emphasis thus upon the higher density carbon-carbons, the focus changed to the precision of the density that the manufacturer could achieve. Some manufacturers would guarantee a precision of only 0.05 to 0.10 gm/cm^3. Added up across 15 cm, these imprecisions could lead to a cumulative error of 0.75 to 1.5 g/cm^2. Some of the aerogels were promising, but the lack of structural properties posed objections, not the least of which was the need to construct some container in which to form and hold it for the beam test.
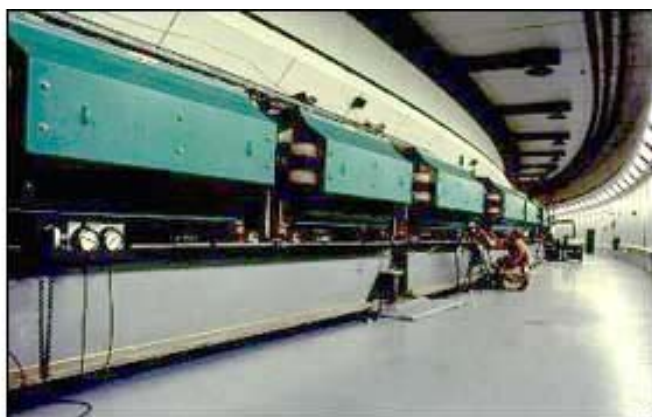

FIGURE 2c. Alternate Gradient Synchrotron circle at Brookhaven National Lab, Courtesy of Brookhaven National Laboratory.

Fortunately, one manufacturer, Carbon-Carbon Advanced Technologies (C-CAT) of Ft. Worth, TX, promised to achieve a density precision of .01 gm/cm^3 in their carbon-filled carbon "CC-1" formulation. Another advantage of the C-CAT product was the availability of excellent and independent NASA thermal test data on very similar formulations from the same manufacturer (Ohlhorst, Vaughn, Ransone, Tsou, 1997, pp. 4-5, 18-19). In addition, a sufficient quantity of CC-1 was affordable on a small budget. On this basis, CC-1 became the material of choice for this experiment. For this experiment, the author specified densification of the phenolic matrix with carbon graphite to 1.65 gm/cm^3. APPENDIX 1 shows the key physical and thermal attributes that C-CAT claims for the CC-1 and thermal properties of the products that NASA-LaRC tested.

PREPARATION OF MATERIALS

C-CAT produced the CC-1 samples on their normal matrix with a nominal thickness of 0.508 cm (0.13in). They produced 24 panels in this thickness, 20 cm x 20 cm square. In order to meet the mass thickness requirement to compose a 5 g/cm^2 shielding unit, it was necessary to machine one panel down to a thickness of 0.490cm. The panels were delivered to Ames Research Center with a coating of graphite dust on all the pieces. There did not appear to be any difference in the graphite dust accumulation on the 0.490cm panels that had been machined to a thinner cross section and the 0.508cm panels that were their original thickness. It was necessary to wash the panels with mild soap to remove the graphite dust. To this panel, the addition of five .508cm thick panels created a sample of 5 g/cm^2.

One such bundle appears in FIGURE 2a. 36mm wide fiberglass-reinforced Scotch "Duct Transparent Tape" held the six panels together in a bundle around their edges. The total production was four bundles to achieve the 20gm/cm^2 sample. These four bundles appear in FIGURE 2b, bound front-to-back with masking tape to keep the pieces upright.

BEAM TIME

On November 10, 2003, the Bioshield Experiment got its "beam time" at BNL. The experiment used 10.5 hours of Fe ions and 7 hours of Ti ions, both from the Alternate Gradient Syncrhotron (AGS), which appears in FIGURE 2c. For both particle types, using the 1 GeV/n particle beam, the absorbed dose ranged from 1 to 20,000 cGy, while the dose rate ranged from 10 to 1,500 cGy/minute. The experiment exposed 60 samples to each of the two beam runs.

RESULTS

The initial results consist of dose reduction measurements and chromosome aberrations per cell in the irradiated lymphocyte culture.

Dose Reduction -- The initial measurements of dose reduction for the 1 GeV/n **Fe** beam through C are encouraging. TABLE 4 shows the measurements in terms of dose per particle, measured in μGy for each of the shielding materials. TABLE 4 shows several important findings. The unshielded incident dose was 0.2300μGy. The Polyethylene performed best in reducing the dose to 0.1290μGy for a reduction of 43.8%.

TABLE 4. Durante and Grossi's results in Dose per Particle for Shielding Materials and Mass "Thicknesses"

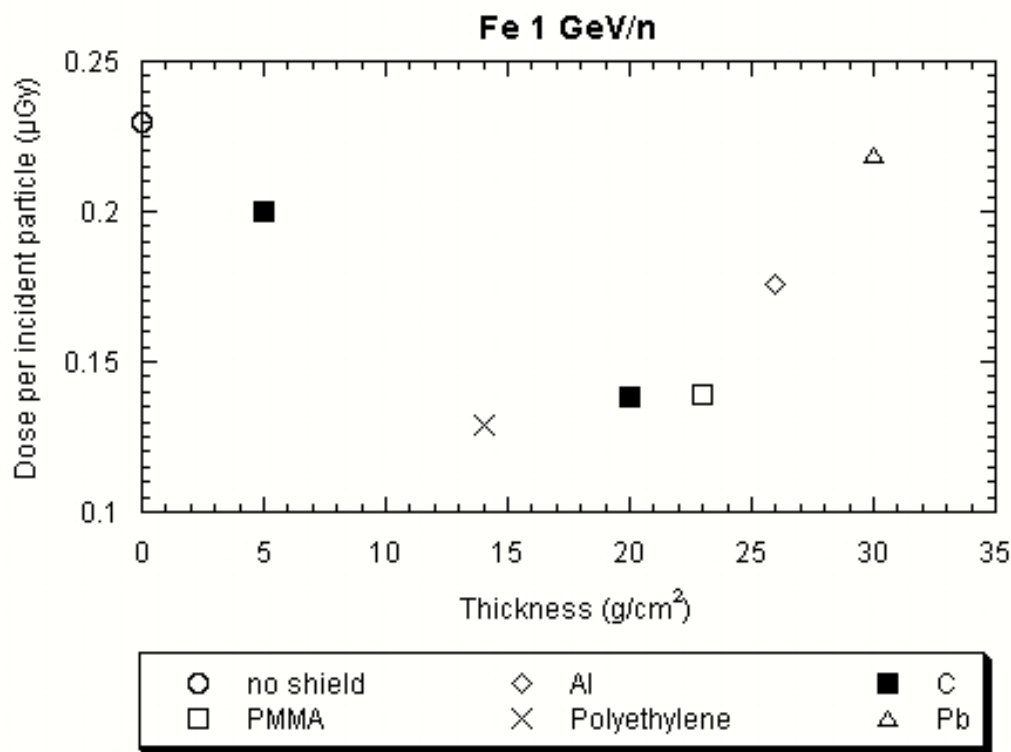| Material Type	Z/A	Front to Back linear thickness in mm	Shielding Mass "Thickness" S_{TH} in g/cm2	Density in g/cm3	Dose per particle in $\mu Gyxcm^2$	Dose Reduction D_R as a Percent of Unshielded Dose	Coefficient of Shielding Mass Effectiveness S_E in Dose Reduction/ Mass Thickness
No shield	-	0	0	-	0.23000	0.00%	0
Polyethylene	0.571	150	14	0.93	0.12900	43.91%	3.136
PMMA Lucite	0.54	190	23	1.2	0.13900	39.57%	1.720
C	0.5	30	5	1.6	0.20000	13.04%	2.608
C	0.5	120	20	1.6	0.13870	39.70%	1.985
Al	0.48	100	26	2.7	0.17600	23.48%	0.903
Pb	0.396	26	30	11.3	0.21000	8.70%	0.290

FIGURE 3. Durante and Grossi's scatter plot of measured radiation dose/particle versus the shielding sample mass "thickness.

When factoring the differences in mass thickness between the 20g/cm² **C** and the 23g/cm² PMMA, the 20g/cm2 **C** shielding performed a comfortable second best overall, with a dose of 0.1387μGy, for a reduction of 39.7%. This result is consistent with Singleterry et al's findings for low energy particles, that polyethylene performs slightly better than composite, and both perform substantially better than aluminum. What is more significant for Habot, however, is the difference between each of the **C** shielding samples and **Al**, the structural material that the Habot project proposes to replace with composite. The 26 g/cm² **Al** reduced the dose to .1760μGy, a reduction of just 23.5%. Although the **Al** mass thickness was more than 25 percent greater than the 20g/cm² **C**, it performed substantially less well. Perhaps even more important was the performance of the 5g/cm2 **C,** which reduced the dose to .2000μGy, a reduction of 13%. This reduction is better than half the **Al** achieved with a mass more than five times greater. FIGURE 3 shows a plot of the dose per particle data in TABLE 4. The quantity reported is the dose per incident particle in an area of 1 cm2. The inverse provides the fluence per unit dose after the shield (in particles/Gy x cm²). An "effective" shield will reduce substantially the

dose/particle behind the shield. **C** has a behavior very similar to polyethylene and PMMA, all these materials being clearly more effective than Al or Pb (obviously the worst). It portrays graphically these results, which are quite dramatic for the comparison of **C** to **Al**. Polyethylene at 30 percent less weight performs slightly better than **C**.

Derived Values -- TABLE 4 includes two columns on the right of simple derived measurements; percent dose reduction and a coefficient of shielding mass effectiveness. These derived values are as simple as possible, but they are useful to compare the performance of the shielding samples overall, factoring out the differences in mass for each different material. Dose reduction percent is D_R,

$$D_R = (D_U - D_S)/ D_U$$

where D_U is the unshielded dose per particle and D_S is the shielded dose per particle.

The coefficient of shielding effectiveness is S_E,

$$S_E = D_R/S_{TH,}$$

where S_{TH} is the Shielding mass thickness. S_E is given in percent dose reduction/g/cm^2.

FIGURE 4a. Support biologist James Jardine prepares one of the NSRL specimen incubators for use. NSRL/BNL Photo.

Chromosome Aberrations – The lymphocytes were isolated from whole human blood by centrifugation. After two washes in PBS medium, the cells were resuspended in RPMI-1640 medium (Gibco-BRL, Grand Island, NY) supplemented with 20% calf serum, and loaded by a syringe into specially constructed 1ml PMMA holders. Both the loading chamber and the holder wall

exposed to the beam are 1 mm thick. The cells were exposed in air at room temperature.

The Bioshield experiment used the novel technique of premature chromosome condensation with phosphatase inhibitors (calyculin A) to visualize the chromosomes in different stages of the cell-cycle22. Immediately after exposure, the cells were transferred to tissue culture flasks in RPMI-1640 medium supplemented with 20% calf serum and 2% phytohaemmaglutinin (PHA, Gibco-BRL, Grand Island, NY). The flasks were incubated in vertical position for 48 h at 37 °C. FIGURE 4a shows a cell incubator at BNL. Calyculin A (Wako chemicals, Japan) at a final concentration of 50 nM was then added for 1 h. Cells containing prematurely condensed chromosomes (PCCs) in G1, S, G2, and M-phase harvested.

To remove residual cytoplasm membrane and organelles, slides were incubated with 100 mg/ml RNase A (Sigma Aldrich) for 1 h at 37°C. After denaturation in 70% formamide/2x SSC (Sigma Aldrich), spreads were hybridized in situ with whole-chromosome DNA probes (Vysis, Downers Grove, IL) specific for human chromosomes 1, 2, and 4, according to manufacturer's instructions. 4,6-diamidino-2-phenylindole (DAPI) in antifade (Vysis) was used as a counterstain. FIGURE 4b shows the cell laboratory at BNL. Durante and Grossi examined the slides through a Zeiss Axioscope epi-fluorescent microscope. All kinds of chromosomal aberrations (dicentrics, translocations, complex-type exchanges, rings, acentric fragments) were scored separately in samples ranging from 150 to 3000 cells per dose (laboratory procedures description courtesy of Durante & Grossi).

FIGURE 4b. Researchers work in one of three NSRL "cell rooms," where samples are prepared for study. NSRL/BNL photo.
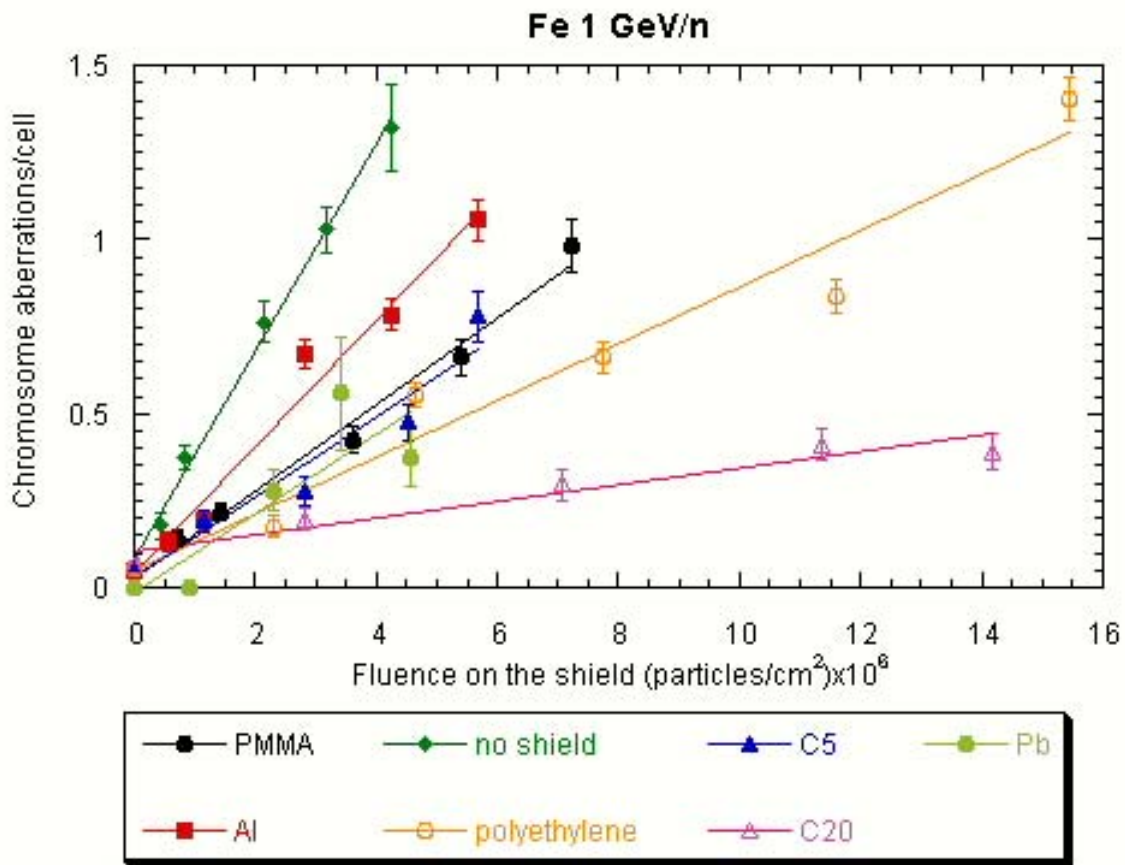
FIGURE 5. Durante and Grossi's Results for Chromosome Aberrations/cell (lymphocyte) for Fe 1 GeV/n.

1. ORNL Carbon Radiator over Thermal Blanket, density and thickness TBD
2. Carbon Filled-Carbon @ 1.65 gm/cm3, .508 cm thick
3. Vitrified Carbon Foam @0.10 gm/cm3 as a structural spacer for micrometeoroid and debris impact protection, 5.00 cm
4. [REPEAT 2 & 3 for up to 5 layers, and to bring the total mass of carbon /cm2.]
5. Pressure vessel shell: ~1 cm of structural epoxy-carbon composite.
6. OPTIONAL Interior LET attenuator, polyethylene, up to 5.00 cm thick
7. OPTIONAL Final neutron absorber, e.g. hafnium, thickness TBD.

FIGURE 6. Representative cross section of a complete Habot wall assembly constructed of carbon composites.

FIGURE 5 shows the biological results for the lymphocytes irradiated under the 1 GeV/n **Fe** beam. FIGURE 5 shows the yield of chromosomal aberrations in human peripheral blood lymphocytes exposed behind the shield. The frequency of aberrations per cell is plotted vs. the fluence of primary Fe ions incident on different shields. FIGURE 5 plots chromosome aberrations against particle fluence through the shielding as the strength of the beam varied.

It appears that 20g/cm2 C-shield provides the highest biological protection. What is surprising about this line chart is how well the two carbon shielding samples perform. The data in FIGURE 3 do not predict these results. The 20g/cm2 C performed far better than the polyethylene, with about 0.30 chromosome aberrations/cell compared to about 1.25 aberrations/cell at the maximum fluence of 14 particles/cm2. *What is most important is that the thinner 5g/cm2 C shielding with about 0.80 aberrations/cell performed better than the 26 g/cm2 Al with about 1.05 aberrations/cell.*

DISCUSSION

This discussion covers four topics: the derived measurements, unexpected results in interpreting the test data, the collaboration between Space Architecture and Biophysics, and the concept of the non-metallic spacecraft and human space habitat. Each of these topics include important but pleasant surprises.

DERIVED MEASUREMENTS

For the purpose of Space Architecture design, it would be most valuable to have a measure of how effective a material is as radiation shielding, independent of mass. Developing this measure, the coefficient of shielding effectiveness, S_E, was an ancillary benefit of the research. From the experimental data, it is simple to compute the percent dose reduction, D_R. Dividing D_R by the shielding mass "thickness" per unit area, S_{TH}, yields the coefficient. Testing aerospace materials for dose reduction and computing the S_E will give a first order approximation of how a material will perform as shielding.

UNPREDICTED RESULTS

From the Space Architecture point of view, there were two expected results: (1) low-energy data would not predict GCR relativistic dose results and (2) that relativistic dose reduction data would predict protection against radiobiological effects. Both expectations proved wrong. This expectation arose from the notion that the metric for biological effects is the rule of thumb in the ICRP space radiation standards concerning the imagined "3 percent excess risk of cancer." However, this "risk" really is based only on data from Low Earth Orbit (LEO). There is no serious risk metric for deep space such as the lunar surface or an interplanetary trajectory to Mars.

The unpredicted or unexpected results were quite pointed. First, there was the apprehension that the low-energy values from Singleterry et al would not predict dose reduction rates for relativistic energy ions. However, despite all of Dr. Singleterry's admonitions and caveats to the contrary, his low energy data do appear to predict the relativistic energy results for risk reduction quite well. Specifically, the low-energy data showed polyethylene performing superior to carbon composite, and carbon composite superior to aluminum. However, the S_E was not a very good predictor of protection against radiobiological effects. In fact, the chromosomal aberration results as shown in FIGURE 4, turned out quite different than the dose reduction data. However, Singleterry explained why the dose reduction data did not predict the biological effects.

> "For a different response function [dose reduction versus biological effects], the [effects of] thickness of shielding can vary greatly. For example, if you look at dose equivalent, then 3-5 g/cm^2 Al is just as good as nothing; however, if you look at cell transformations, then you need 30+ gm/cm^2 of Al to be just as good as nothing. The design requirement for radiation is a fatal cancer risk over the base population of 3% . . . . However, cell transformation matches cancer rates in real biology. . . . Therefore, dose equivalent is not a good measure of the design risk" (personal communication via e-mail from Robert Singleterry, April 27, 2004).

Fortunately, the unexpected result went in the favorable direction that the 20g/cm^2 **C** performed significantly better than 14g/cm^2 polyethylene. The most dramatic result was that the 5gm/cm2 C performed better than the 26g/cm2 Al.

NON-METALLIC, COMPOSITE SPACE HABITAT

The most compelling outcome of this research is that it provides a foundation for designing an entirely non-metallic space habitat. With the radiation protection data from the Bioshield experiment, it becomes clear that an all carbon composite habitable spacecraft structure, including pressure vessel, thermal insulation, radiation shielding, and body-mounted radiators would have persuasive advantages over aluminum alloys.

Exterior Protective Layers -- FIGURE 6 illustrates an example of a possible Habot wall cross-section. The outermost layer appears at the top of the figure, with a body-mounted thermally conductive radiator (Klett, 1998). Under the radiator, and wrapping the module except for windows is a conventional "silvered" kapton foil thermal blanket to reduce thermal radiative heat gain

and loss. It will be necessary to test these foils for secondary neutron production before making a material selection. Under the thermal blanket would be alternating layers of high-density carbon-filled carbon and lightweight, highly insulating vitrified carbon foam, up to the desired total section thickness. This alternate layering provides radiation shielding, thermal insulation and micrometeoroid protection.

Pressure Vessel and Interior Outfitting – Under these alternating protective layers is the structural composite pressure vessel, composed of a highly reliable epoxy composite. This pressure vessel serves three purposes: it holds the atmosphere for the habitat, it provides hard points to support the external protective material and it provides hard points to support interior secondary structure such as stand-offs for racks and floors. Inside the pressure vessel, with further testing, it may be helpful to install a dedicated LET absorber of boronated polyethylene and possibly a final neutron absorber such as a thin layer of hafnium. The use of such terminal protections would depend largely upon the ability of the protective layers to reduce the energy level of neutrons to the best efficacy levels of the terminal materials.

Full Wall Assembly Testing – The key to successful development of the all-carbon protective layers and pressure vessel system for Habot is to test complete wall assemblies for each of the environmental demands made upon it. These integrated wall assembly tests must include more radiation beam testing, ballistic projectile testing for micrometeoroid impact, and thermal vacuum testing under the lunar day-night cycle.

PROOF OF CONCEPT

Although the chromosome aberration measurements are only one aspect of Bioshield experiment, they appear to provide **_Proof of Concept_** for the Carbon shielding, demonstrating that it outperforms its rivals – at least for one particle at one energy -- on the measure that counts most: to protect human crew members. This proof of concept which gives it a NASA Technology Readiness rating of TRL 3 on a scale of 0 to 9. APPENDIX 2 presents a table that explains the NASA Technology Readiness Scale (TRL). This proof of concept of carbon as a shielding material defines a new starting point for developing carbon composite as a material for building human spacecraft.

Moving Up the Scale to TRL-4 -- The follow-up steps to develop carbon shielding to higher levels on the TRL scale will involve a variety of further tests and advances in design. The next step to bring it to TRL 4 should involve testing more formulations of carbon at differing (mostly lesser) densities, and testing a realistic and practical habitat (i.e. Habot) wall section. This wall section would reflect the cross section described in FIGURE 6.

Achieving TRL-4 should also include early space exposure testing of small samples of each of the various materials. Ideally, this experiment would involve attaching an exposed payload carrier to an external exposure experiment platform on ISS.

Beyond TRL-4 -- To achieve TRL 5, the testing should extend to other environmental stressors such as thermal and pressure differentials, ballistic impact testing, and electrostatic arc experiments. To achieve TRL 6 would involve constructing a complete subscale composite pressure vessel with the all-carbon external wall assembly, then instrumenting it extensively with sensors for structural, thermal-vacuum, pressure and other forms of testing. To achieve TRL 7 would involve taking a complete sub-scale test article based upon the TRL 7 experience and results, adding radiation dosimetry sensors, and launching it on a flight experiment into cislunar space. It would be necessary to place the experiment into lunar orbit for some period of months, and then return it to the Earth for examination and detailed structural and materials science evaluation. Once the carbon shielding/composite habitat technology succeeds in such a flight experiment, NASA will be ready to build a full scale, operational Habot habitat, space-qualified for landing on the moon and human rated for the crew to occupy it there.

MULTIDISCIPLINARY COLLABORATION

The cooperation between Space Architecture Design Research with Biophysics in radiation research was a fruitful collaboration. The two disciplines came together from totally different perspectives on the radiation-shielding problem. Working together, they produced a result far better than either would have expected. This collaboration led to some new ideas and even new ways of thinking for the collaborators. There were a few surprises along the way. The fact that the Habot Project was the only contributor of shielding that adhered strictly to the specifications was one such surprise. For future experiments, it would be most helpful to have similar precision in the mass thickness of all the shielding samples. On the other hand, the fact that the co-authors could distill compelling results despite the disparities in shielding thickness is most reassuring.

CONCLUSION

The relativistic beam test measurements showed that carbon-carbon shielding is competitive with polyethylene and PMMU/Lucite for reducing incident doses of particle radiation. The same test showed that carbon-carbon is superior to aluminum alloy as a shielding material. The most surprising result was the superior performance of carbon-carbon at reducing chromosome aberrations in the lymphocyte culture. However, nobody should think that there is anything clever in the application and testing of carbon-carbon as a radiation shielding material. The

"walk through the periodic table" shows that carbon is an obvious candidate for testing as a shielding material. The caveat on these results is that they apply to one particle in one energy range for one biological measure. However, the results of this experiment provide a clue of good performance of carbon as a shielding material and justify further experiments with this material.

If it proves possible to extend the narrow results of this experiment to the full spectrum of particles and energies, the meaning of these results for Space Architects, Designers, and Engineers will be profound. Such an outcome would suggest that an entirely non-metallic composite spacecraft and space habitat offers performance capabilities, both in terms of radiation shielding, thermal insulation, and mass reduction that are superior to aluminum alloys.

DEDICATION

This study is dedicated to Delbert Philpott, Ph.D., my neighbor 1993-1991 across the hall in the basement of Building N-239, Ames Research Center. Del was a hero in WWII – one of the first three US soldiers to link up with the Russians at the River Elbe, and a pioneer in the study of radiobiological damage from GCRs. He first interested me in the problem of radiation protection.

ACKNOWLEDGMENTS

REFERENCES

Ballarini, F.; Merzagora, M.; Monforti, F.; Durante, M.; Gialanella, G.; Grossi, G. F.; Pugliese; M.; Ottolenghi, A. (1999) Chromosome aberrations induced by light ions: Monte Carlo simulations based on a mechanistic model. *Int. J. Radiat. Biol. 75*, p. 35-46.

Cohen, Marc M. (1996). Design of a Planetary Habitat Versus an Interplanetary Habitat. *SAE Transactions, Journal of Aerospace*, Vol. 105, Section 1, p. 574-599. Warrendale, Pennsylvania, USA: Society of Automotive Engineers.

Cohen, Marc M. (1997). Design Research Issues for an Interplanetary Habitat. *SAE Transactions, Journal of Aerospace*, Vol. 106, Section 1, p. 967-994. Warrendale, Pennsylvania, USA: Society of Automotive Engineers.

Cohen, Marc M. (2003) "Mobile Lunar and Planetary Bases," AIAA-2003-6280, *AIAA Space 2003 Conference*, San Diego, CA, Sept. 23-25, 2003. Reston VA: AIAA.

Cohen, Marc M., (2004). "Mobile Lunar Base Concepts," 2004-STAIF-291, *2004 Space Technology and Applications International Forum*, Albuquerque, NM, Feb. 8-11, 2004, College Park, MD: American Institute of Physics.

Cohen, Marc M.; Kennedy, Kriss J. (1997, November). "Habitats and Surface Construction Technology and Development Roadmap," in A. Noor, J. Malone (Eds.), *Government Sponsored Programs on Structures Technology*, NASA CP-97-206241, p. 75-96. Washington, DC, USA: National Aeronautics and Space Administration.

Durante, M.; Bonassi, S.; George, K.; Cucinotta, F.A. (2001). Risk estimation based on chromosomal aberrations induced by radiation. *Radiation Research 156,* p. 662-671.

Durante, M. ; Furusawa, Y. ; Gotoh, E. (1998). A simple method for simultaneous interphase-metaphase

chromosome analysis in biological dosimetry. *Int. J. Radiat. Biol. 74*. p. 457-462.

Durante, M. (2000) Italian Space Radiobiology Program: influence of the shielding on the biological effects of heavy ions. In Majima, H.; Fujitaka, K. (Eds.), *Exploring Future Research strategies in Space Radiation Sciences* , Tokyo: Iryokagakusha. p.79-85.

Lai, A. Yip Hung; Howe, A. Scott, (2003) "A Kit–of-parts Approach to Pressure Vessels for Planetary Surface Construction," AIAA-2003-6281, *AIAA Space 2003 Conference*, San Diego, CA, Sept. 23-25, 2003. Reston VA: AIAA.

Mankins, John C., "Modular Architecture Options for Lunar Exploration and Development," IAA.13.2.05, *51st International Astronautical Congress,* Rio de Janeiro, Brazil. October 2-6, 2000, Paris, France: IAA.

Mankins, John C., (2001). "Modular Architecture Options for Lunar Exploration and Development," *Space Technology,* 21, pp. 53-64.

NASA, Life Sciences Division (1999) Strategic Program Plan for Space Radiation Health Research Washington DC: NASA.

Ohlhorst, Craig W.; Vaughn, Wallace L., Ransome, Philip O.; Tsou, Hwa-Tsu (1997, November). Thermal Conductivity Database of Various Structural Carbon-Carbon Composite Materials, NASA TM-4787. Hampton VA: NASA Langley Research Center.

Sapp, W.J.; Philpott, D.E.; Williams, C.S.; Williams, J.W.; Kato, K.; Miquel, J.M., Serova, L. (1988) "Comparative Study of Spermatological Survival after X-Ray Exposure, High LET (HZE) Irradiation or Spaceflight," *Advances in Space Research,* Vol 12, No. 2-3, pp. (2) 179-(2) 189.

Simonson, Lisa C. (1997) Evaluation of a charge coupled device (CCD) for use as a nuclear charged particle detector for space applications, PhD Dissertation, Charlottesville VA: University of Virginia.

Simonson, Lisa C., Nealy, John E., Townsend, Lawrence W., & Wilson, John W., (1990, March). Radiation Exposure for Manned Mars Surface Missions, NASA TP 2979, Washington DC: NASA.

Simonson, Lisa C.; Nealy, John E. (1991, February). Radiation Protection for Human Missions to the Moon and Mars, NASA TP 3079, Washington, DC: NASA.

Singleterry, Jr., Robert C.; Thibeault, S.A. (2000, June) Materials for Low-Energy Neutron Radiation Shielding, NASA/TP-2000-210281, Washington DC: NASA.

Singleterry, Jr., Robert C.; Thibeault, S.A.; Wilkins, R.T.; Huff, H. (2002). "Charged and Neutral Particle Interactions on Aerospace Materials," *International Congress on Advanced Nuclear Power Plants,* June 9-13, 2002, Hollywood, FL.

Townsend, Lawrence W., Nealy, John E., Wilson, John W., Simonson, Lisa C., (1990, February). Estimates of Galactic Cosmic Ray Shielding Requirements During Solar Minimum, NASA TM 4167, Washington DC: NASA.

Wilson, J. W.; Cucinotta, F. A.; Miller, J.; Shinn, J. L.; Thiebeault, S. A.; Singleterry, R. C. Jr.; Simonson; L. C.; Kim, M. H. (1998). "Materials for Shielding Astronauts From the Hazards of Space Radiations," *Materials Research Society Fall Meeting,* Boston MA, November 30-December 4, 1998.

CONTACT

Marc M. Cohen, Arch.D, Architect
Advanced Projects Branch
Mail Stop 244-14
NASA-Ames Research Center
Moffett Field, CA 94035-1000 USA
TEL +1 650 604-0068
FAX +1 650 604-0673
Marc.m.cohen@nasa.gov

Prof. Marco Durante, Ph.D.
Dipartimento di Scienze Fisiche, Università di Napoli "Federico II"
Monte S. Angelo, Via Cynthia, 80126 Napoli, ITALIA
TEL   +39 081 676- 440 (off.)
TEL   +39 220 -294 -296 (lab.)
FAX   +39 081 676 346
Marco.Durante@na.infn.it

Gianfranco Grossi, PhD
Professor of Physics and Biophysics
Dipartimento di Scienze Fisiche, Università di Napoli "Federico II"
Complesso Universitario Monte Sant'Angelo,
 I-80126 Napoli ITALIA
TEL   +39 08167 6277
FAX   +39 08167 6346
CEL   +39 33537 7508
Gianfranco.Grossi@na.infn.it

ADDITIONAL SOURCES

Benaroya, Haym, "An Overview of Lunar Base Structures: Past and Future," AIAA 2002-6113, *1st AIAA Space Architecture Symposium (SAS 2002),* Houston, Texas, USA, 10-11 October 2002. Reston, VA: AIAA.

Cohen, Marc M., "First Mars Outpost Habitation Strategy," in C. Stoker,. C. Emmart, Eds. Strategies for Mars: A Guide for Human Exploration, *Vol 86, AAS Science and Technology Series*, San Diego, CA: Univelt. 1996.

Cohen, Marc M., Space Habitat Design Integration Issues SAE 981800. *28th International Conference on Environmental Systems* (ICES), Danvers, MA, 13-16 July 1998. Warrendale, PA: SAE.

Commission on Atomic Weights and Isotopic Abundances report for the International Union of Pure and Applied Chemistry in Isotopic Compositions of the Elements 1989, Pure and Applied Chemistry, 1998, 70, 217. [Copyright 1998 IUPAC]

Durante, M. ; et al., (2001) Space radiation shielding: biological effects of accelerated iron ions and their modification by aluminum or lucite shields. *Micrograv. Space Stat. Utiliz. 2* (2001) 432-437.

Durante, M.; Grossi, G.; Pugliese, M.; Gialanella, G. (1996). Nuclear track detectors in cellular radiation biology. *Radiation Measurments.*,*13*. p. 34-44.

International Commission on Radiation Protection, ICRP (1991) Recommendations of the International Commission on Radiological Protection. *Annals of the ICRP 21,* Publication 60, Oxford UK: Pergamon Press.

Mills, T. Cvitas, K. Homann, N. Kallay, and K. Kuchitsu in (1998). Quantities, Units and Symbols in Physical Chemistry, Blackwell Scientific Publications, Oxford.

Setlow, Richard, et al, Radiation Hazards to Crews of Interplanetary Missions: Biological Issues and Research Strategies, (1996). Space Studies Board – National Research Council, Washington DC: National Academy Press.

Singleterry, Jr., Robert C.; Badavi, F.F.; Shinn, J.L.; Cucinotta, F.A.; Badhwar, G.D.; Clowdsley, M.S.; Heinbockel, J.H.; Wilson, J.W.; Atwell W.; Beaujean, R.; Kopp, J.; Reitz, G. (2001, June). "Estimation of Neutron and Other Radiation Exposure Components in Low Earth Orbit," *Radiation Measurements*, Vol. 33, No. 3.

Task Group on the Biological Effects of Space Radiation, National Academy of Sciences (1996) Radiation Hazards to Crews of Interplanetary Missions: Biological Issues and Research Strategies, NRC, Washington DC: National Academic Press.

Townsend, Lawrence W., Wilson, John W., Nealy, John E., (1988, October). Preliminary Estimates of Galactic Cosmic Ray Shielding Requirements for Manned Interplanetary Missions, NASA TM 101516, Hampton VA: NASA.

Vazquez, Marcelo E. (2004, January) NSRL-1 Run Final Report, Upton NY: Brookhaven National Laboratory.

Wilson, J.W., Miller, J., Konradi, A., Cucinotta, F.A., Eds. *Shielding Strategies for Human Space Exploration,* NASA CP-3360, Hampton, VA: NASA. Dec. 1997.

DEFINITIONS, ACRONYMS, ABBREVIATIONS

AIAA — American Institute of Aeronautics and Astronautics.

ARC — NASA Ames Research Center

BNL — Brookhaven National Laboratory, US Department of Energy, Upton, NY

C-CAT — Carbon-Carbon Advanced Technologies, Inc., Ft. Worth, TX USA

CC-1 — carbon-filled carbon composite

CEV — Crew Exploration Vehicle, *Project Constellation*

CGY — centiGray, the S.I. equivalent of 1 RAD.

GCR — galactic cosmic ray particle

GeV/n — giga electron volt

Gy — Gray, unit of absorbed radiation dose. 1 cGy equals 1 RAD.

HZE — Heavy Z particle, typically a helium nuclei or larger

IAA — International Astronautics Academy

IAC — International Astronomical Congress

ICRP — International Commission on Radiation Protection

JSC — NASA Johnson Space Center, Houston, TX

kgf/m^2 — kilogram force/square meter

LANL — Los Alamos National Laboratory, US Department of Energy, Los Alamos, NM

LANSCE — Los Alamos Neutron Science Center

LaRC — NASA Langley Research Center, Hampton, VA

LET — linear energy transfer

MeV — mega electron volt

$\mu Gy/cm^2$ — micro-Gray / centimeter square, the unit of relativistic particle dose.

MPa — Mega pascal

MSDS — Material Safety Data Sheet

MSFC — NASA Marshall Spaceflight Center

NASA — National Aeronautics and Space Administration

NCARR — NASA Center for Applied Radiation Research at PVAMU

NRC — National Research Council

NSRL — NASA Space Radiation Laboratory, at Brookhaven, Upton, NY

ORNL — Oak Ridge National Laboratory, US Department of Energy, Oak Ridge, TN

PMMA — polymethyl methacrylate, a formulation of acrylic/Lucite

PVAMU   Prairie View Agriculture and Mechanics
         University, Prairie View, Texas

RBE   Radiobiological effect

SAE   Society of Automotive Engineers

Z/A   Atomic Number/Atomic Weight

APPENDIX 1: PROPERTIES OF CARBON-FILLED CARBON

MANUFACTURER'S DATA

PRODUCT NAME: C-CAT   CC-1 (F-3)

REINFORCEMENT: (CC-1) Heat-treated Amoco T-300 fiber. 3k yarn 8 Harness satin weave

FIBER VOLUME: (CC-1) Approximately 55%

MATRIX PRECURSOR: Phenolic Resin

TYPE OF PROCESSING:
Densification by phenolic resin impregnation.
SiC coating by pack cementation.

THERMAL PROPERTIES

RECOMMENDED USE TEMPERATURE

IN AIR:
(Long term) Uncoated 370° C,
Uncoated maximum, 540°C, 10 hrs.
1% weight loss for heat-treated

(Long term) Coated 370° to 1425°C isothermal

INERT: 2760°C

IN VACUUM: 2200 °C

AVERAGE THERMOPHYSICAL PROPERTIES

DENSITY: 1.65 gm/cc for carbon filled

COEFFICIENT OF THERMAL EXPANSION (SPECIFY TEMPERATURE RANGE):
1. (Warp) 0.9e+06mm/mm°C (20 to 1650°C)
2. (Fill) 0.9e+06 mm/mm°C (20 to 1650°C)
3. (Across ply) 6.3e+06 (20 to 1650°C)

THERMAL CONDUCTIVITY (SPECIFY RANGE): At 3000°F = 1650°C
K1. (Warp) = 36.05 W/m°C
K2. (Fill) = 36.05 W/m°C
K3. (Across ply) 5.047W/m°C

SPECIFIC HEAT (SPECIFY TEMPERATURE):
1,884J/kg-°C @ 1650°C

ROOM TEMPERATURE MECHANICAL PROPERTIES

ELASTIC CONSTANTS:

E_1, E_2 (tension) & E_1, E_2 (compression) = 9.84297e+09 kilogram-force per square meter (kgf/m^2) or 96,526.6 megapascal (MPa).

E_3 (tension), E_3 (compression) = 4.92149e+08 kgf/m^2 or 4,826.33 (MPa)

STRENGTH

Tensile ultimate = 3.16381e+07 kgf/m^2 or 310.264 (MPa).

Compressive ultimate = 1.75767e+07 kgf/m^2 or 72.369 MPa

Flexure ultimate = 2.67166e+07 kgf/m^2 or 262.001 MPa.

Shear ultimate = 3.79658e+06 kgf/m^2 or 37.2317 MPa.

1 (tensile ultimate) = 0.3% (21°C), 0.6% (1650°C)

1 (compressive ultimate) = 0.15% (21°C), 0.35% (1650°C).

INTERLAMINAR TENSILE STRENGTH:

(25mm diameter button) 421,842 kgf/m^2 or 4.13685 MPa

INTERLAMINAR SHEAR STRENGTH:

703,070 kgf/m^2 or 6.89476 MPa at 21°C (double notch)

1.40614e+06 kgf/m^2 or 72.369 MPa at 1650°C (double notch)

APPENDIX 1, TABLE 1. NASA LANGLEY INDEPENDENT THERMOPHYSICAL TEST DATA

Ohlhorst, Craig W.; Vaughn, Wallace L., Ransome, Philip O.; Tsou, Hwa-Tsu (1997, November). <u>Thermal Conductivity Database of Various Structural Carbon-Carbon Composite Materials,</u> NASA TM-4787. Hampton VA: NASA Langley Research Center. p 18-19.

Material Specimen	Density g/cm3	Direction	Temperature °C	Heat Capacity J/g-K	Thermal Diffusivity cm^2/s	Thermal Conductivity W/m-K	Note
C-CAT T-300 3k Phenolic Densified Material.	1.593	In-plane	18	0.674	0.208	22.349	1
			126	0.988	0.178	28.016	
			205	1.172	0.159	29.673	
		t-t-t	`18	0.674	0.013	1.397	
			127	0.991	0.0128	2.020	
			205	1.172	0.0126	2.351	
Type III Coated C-CAT T-300 3k Phenolic Densified Material	1.814	t-t-t	18	0.681	0.0293	3.620	2
			127	0.988	0.0252	4.516	
			205	1.174	0.0243	5.175	
		t-t-t re-measured	20	0.681	0.0293	3.620	
			126	0.988	0.0252	4.516	
			206	1.174	0.0243	5.175	

t-t-t = through the thickness of the material

Note 1. Conductivity values provided by NASA-LaRC in NASA TM-4787.

Note 2. Conductivity values computed by the author for the thermal conductivity k, given that $k = \alpha \alpha c_p$, where α is the density, α is the thermal diffusivity, and c_p is the heat capacity (specific heat).

Description of Development	NASA Technology Readiness Level (TRL)	Colloquial Term	Habot Dev. Cycle
System Test, Launch and Operations	**9. Actual system "flight proven" through successful mission operations** (Operational Test and Engineering -- OT&E).	Flight Test	4
System /Subsystem Development	**8. Actual system completed and "flight qualified" through test and demonstration** (ground/flight test / Design, Development, Test and Engineering --DDT&E).	Flight Qualification Test	3
Technology Demonstration	**7. Systems prototype demonstration in a flight/space environment** (System Prototype Test in Operational Environment).	Operational Environment Test	
	6. System/subsystem model or prototype demonstration in a relevant environment (Prototype Test in Relevant Environment).	Prototype or Environmental Test	2
Technology Development	**5. Component and/or breadboard validation in a relevant environment.** (Breadboard Integration)	Breadboard Test	
	4. Component and/or breadboard validation in laboratory environment. (Breadboard Integration)	Lab Test	1
Research to Prove Feasibility	**3. Analytical and experiment critical function and/or characteristic proof of concept** (Component Development).	Proof of Concept	
Basic Technology Research	**2. Technology concept and/or application formulated** (Invention)	Invention	
	1. Basic principle observed and reported (Paper Study)**.**	Discovery	